Jurnal Mekanikal, Jilid II, 1996

HEAT TRANSFER AND STRENGTH ANALYSIS OF COLUMN AT EXTREME TEMPERATURE

Badri Abdul Ghani
Mohamed El-Shayeb

Department of Applied Mechanics
Faculty of Mechanical Engineering
Universiti Teknologi Malaysia

T.T.Lie
Division of Building Research
National Research Council, Canada

ABSTRACT

Experimental and theoretical studies have been carried out to predict the fire resistance of protected I-shaped steel insulated with ceramic fibre. A mathematical model to calculate the temperatures, deformations and fire resistance of the columns have been presented in this paper. The model enables the expansion of data on the protected steel columns involving ceramics which at present, consists predominantly with data for concrete columns.

1. 0 INTRODUCTION

The use of I-shaped structural steel sections has several benefits as such sections are structurally very efficient in resisting compression loads and bending loads. In addition, a high fire resistance can be obtained without the necessity of external fire protection for the steel and the addition of ceramic protection or other insulation will enhance it further. These benefits have stimulated the use of such steel columns.

The columns that are under study are made of structural steel section that is classified as Wide-flange steel sections under the materials code - the Canadian Standards Association, CSA G40.21-M81. As protection against extreme heat, the steel sections are fully covered in ceramic blanket, which follow the contour of the steel section. Several section sizes have been initially identified as possible candidates for the test ranging from the smaller W250-49 to the larger W310-158. Eventually two sections, W250-80 and the W310-158 were selected for the experimental verifications. The reason for having two vastly different sizes is to ensure variability in the test data so as to produce reliable validation. A specimen utilising the W250-80 I-shaped steel section covered with ceramic fibre is shown in Fig. 1 and Fig. 2.

2.0 HEAT TRANSFER MATHEMATICAL MODEL

Calculation of the fire resistance of the column is carried out in various steps. It involves the calculation of temperatures of the fire to which the column is exposed, temperatures in the column, and the column deformations and strength during its exposure to fire. The column temperatures are calculated by using finite-difference method [5]. This paper will discuss only the developed equations for the calculation of column temperatures and strength.

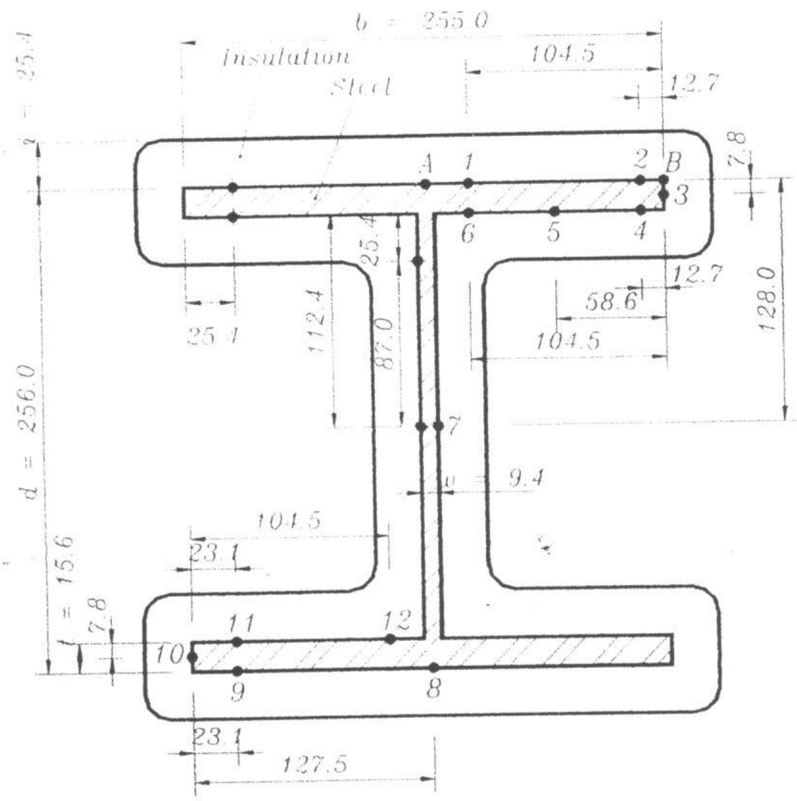

Fig. 1 W250-80 Steel Section with 1 inch Ceramic

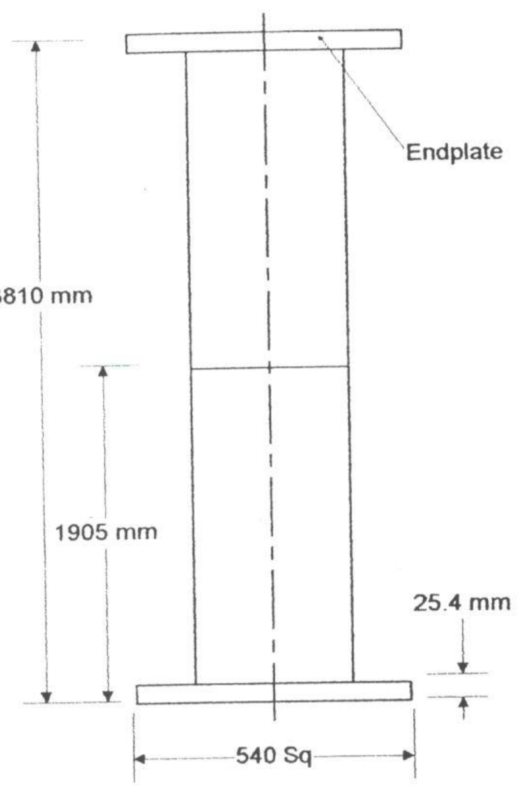

Fig. 2 The Length of Beam

2.1 Division of Cross Section into Elements

As the column is double-symmetrical, it can be represented by only one quarter of its cross-section in the calculation of the temperature distribution as shown in Fig. 3. The cross-section of the column is subdivided into meshes of elements and nodes, arranged in a network sloped at 45° to the horizontal as seen in Fig. 4. The elements are square inside the column and triangular at the surface. For the square elements, the temperature at the centre node is representative of the temperature of the whole element. For the surface triangular elements, the representative nodes are located on the centre of the hypotenuse.

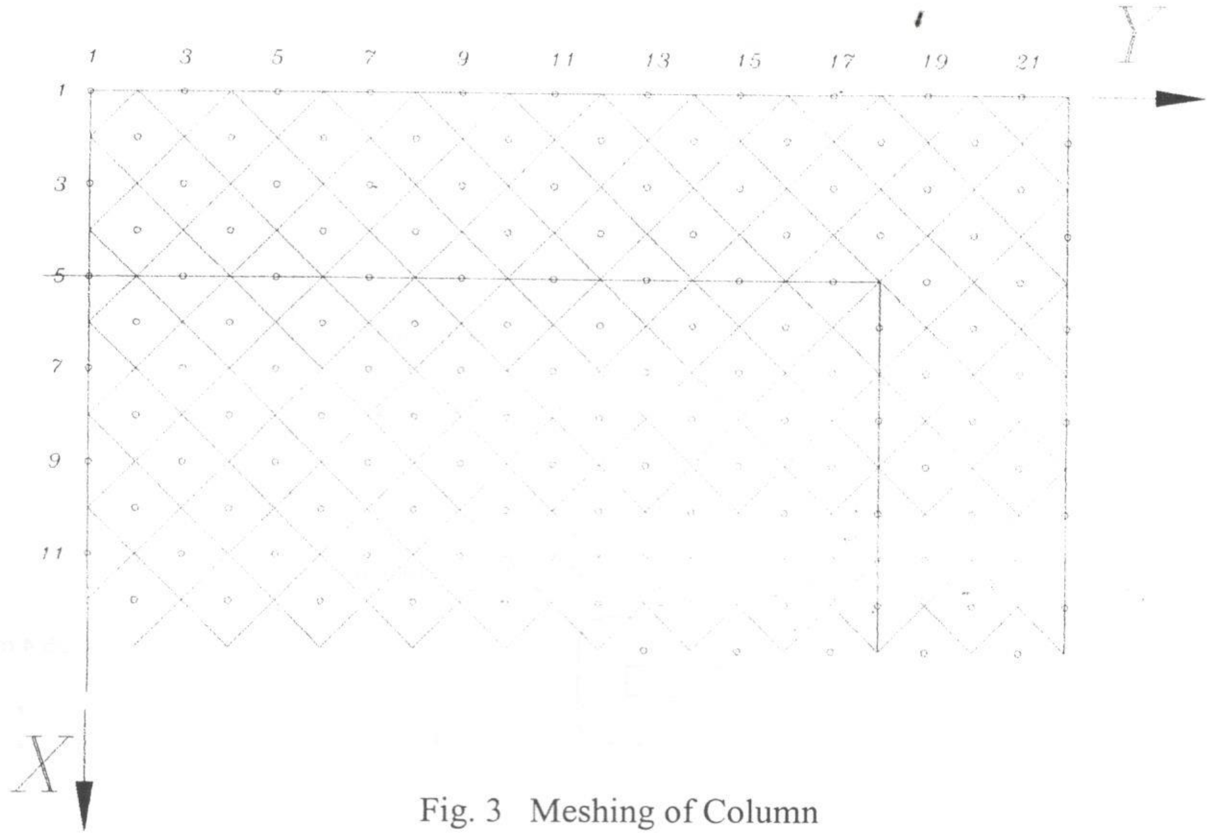

Fig. 3 Meshing of Column

The cross-section are located on a set of X-Y co-ordinate axes with a virtual matrix axes M,N representing nodal points and the origin 0,0 at X-Y axes will start with (1,1). Each (m,n) points are located at $x = (m-1)\,\Delta\xi/\sqrt{2}$ and $y = (n-1)\Delta\xi/\sqrt{2}$ and $m = M$ and $n = N$ is the maximum distance that can be attained along the X and Y axis.

Due the more complicated shape of the I-beam there are several boundaries needed for the mathematical-modelling of the column. For calculation of temperature in the whole column, a total of eight different boundary conditions have been identified as shown in Fig. 4. Three are located at the wall surfaces, three in the border of insulation of steel beam and one each in the insulation region and steel region.

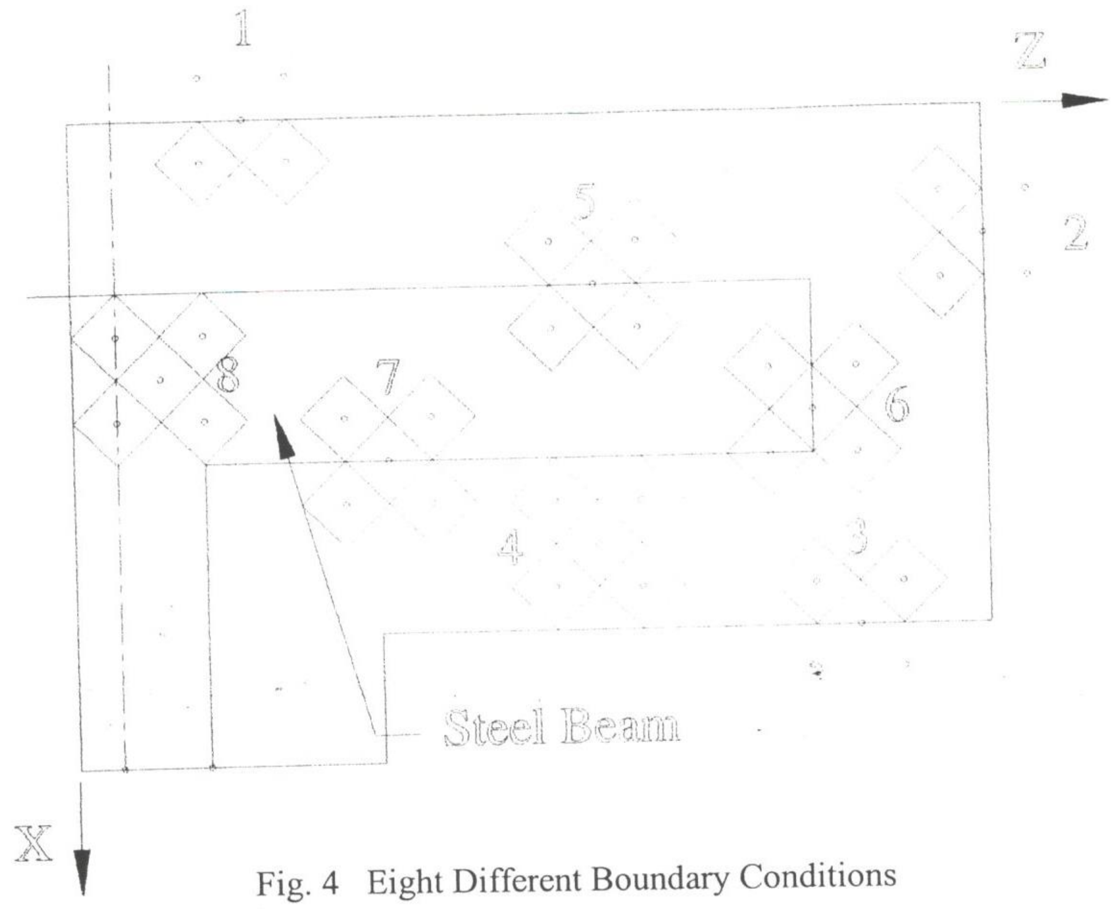

Fig. 4 Eight Different Boundary Conditions

2.2 Assumptions in heat transfer mathematical model

1. It is assumed that the heat distribution along the length of the column is equal.
2. It is assumed that heat transfer by convection is negligible.

The first criteria assumes that heat distribution along the column length is equal and each plane of cross-section of the column experiences equal heat flow from the ceramic wall surface to the inner steel core, thus the developed mathematical model will be 2-dimensional. The flow by convection will result in minimal increase in the rate of heat energy reaching the column core.

2.3 Fire - Insulation Boundary (Case 1)

This is the region when heat is absorbed into the column from the scorching fire through the wall made of ceramic fibres. Because of the inherent quality of ceramic, heat is transferred at slow rate across the depth of the insulation. The emissivity of ceramic is given as 0.6 and that of fire estimated to be 0.9 that is very closed to a perfect "black body".

In the first heat-balance case involving column boundary, the fire is at the upper side of the 5-nodes mesh and ceramic wall is at the lower side. The heat is transferred by radiation from fire through the wall surface and is transferred deeper into the column's wall by conduction. The simulated case is shown in Fig. 5 and the calculation as shown below:

Heat is transferred by radiation through the wall surface and from the equation of heat radiation, the following expression is obtained,

$$q_r = A_{fs}\sigma\varepsilon_f\varepsilon_c\left[\left(T_f^j + 273\right)^4 - \left(T_{m,n}^j + 273\right)^4\right]$$

where q_r is the heat transferred by radiation , $J/_{m.hr}$ and

A_{fs} is the surface area of the element exposed to fire $=$ $2(\Delta h_g)(1.0)$

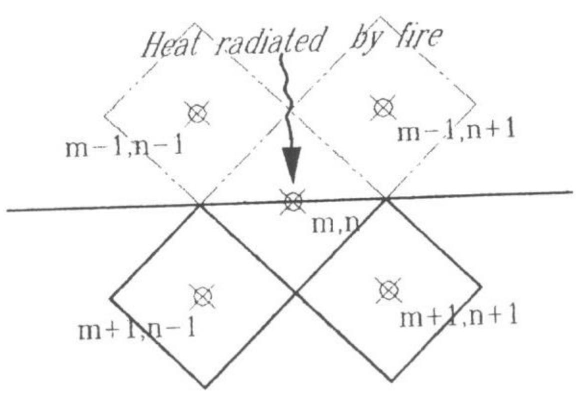

Fig. 5 Case 1

Heat transfer into the wall is given by the following 2-dimensional partial differential equation:

$$\left\{\left[\frac{\partial}{\partial x}K\frac{\partial T}{\partial x}\right]_{m,n}^{j}+\left[\frac{\partial}{\partial y}K\frac{\partial T}{\partial y}\right]_{m,n}^{j}\right\}A_{el}=\left\{\left[\rho C\frac{\partial T}{\partial t}\right]_{m,n}^{j}\right\}A_{el}$$

Combining all the terms in the Sensible Heat equation, $q_1 - q_2 = \dfrac{\partial E}{\partial t}$

And by applying the finite difference technique to the above equations, we can get the fire-insulated boundary as follows:

$$T_{m,n}^{j+1}=T_{m,n}^{j}+\frac{\Delta t}{\left[\rho_c C_c\right]_{m,n}^{j}\Delta h_g^2}\cdot\left\{2\Delta h_g\sigma\varepsilon_f\varepsilon_c\left[\left(T_f^j+273\right)^4-\left(T_{m,n}^j+273\right)^4\right]+\right.$$
$$\left.\frac{1}{2}\left[\left(K_{C_{m,n}}^j+K_{C_{m+1,n-1}}^j\right)\left(T_{m+1,n-1}^j-T_{m,n}^j\right)+\left(K_{C_{m+1,n+1}}^j+K_{C_{m,n}}^j\right)\left(T_{m+1,n+1}^j-T_{m,n}^j\right)\right]\right. \tag{1}$$

This is the heat balance equation at the column surface as the heat is radiated from fire into the wall.

2.4 Fire - Insulation Boundary (Case 2)

Heat sources from the right side of the column (see Fig. 6) can be derived in a similar method to get the following expression:

$$T_{m,n}^{j+1}=T_{m,n}^{j}+\frac{\Delta t}{\left[\rho_c C_c\right]_{m,n}^{j}\Delta h_g^2}\cdot\left\{2\Delta h_g\sigma\varepsilon_f\varepsilon_c\left[\left(T_f^j+273\right)^4-\left(T_{m,n}^j+273\right)^4\right]+\right.$$
$$\left.\frac{1}{2}\left[\left(K_{C_{m,n}}^j+K_{C_{m+1,n-1}}^j\right)\left(T_{m+1,n-1}^j-T_{m,n}^j\right)+\left(K_{C_{m-1,n-1}}^j+K_{C_{m,n}}^j\right)\left(T_{m-1,n-1}^j-T_{m,n}^j\right)\right]\right. \tag{2}$$

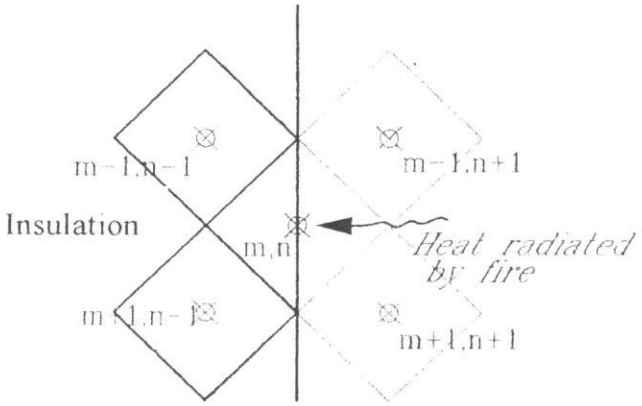

Fig.6 Case 2

2.5 Fire - Insulation Boundary (Case 3)

In the third boundary case, heat flow is from the back side of the column as shown in Fig. 7, then the resulted boundary equation is:

$$T_{m,n}^{j+1} = T_{m,n}^{j} + \frac{\Delta t}{\left[\rho_c C_c\right]_{m,n}^{j} \Delta h_g^2} \cdot \left\{ 2\Delta h_g \sigma \varepsilon_f \varepsilon_c \left[\left(T_f^j + 273\right)^4 - \left(T_{m,n}^j + 273\right)^4 \right] + \right.$$

$$\left. \frac{1}{2} \left[\left(K_{C_{m-1,n+1}}^{j} + K_{C_{m,n}}^{j}\right)\left(T_{m-1,n+1}^{j} - T_{m,n}^{j}\right) + \left(K_{C_{m-1,n-1}}^{j} + K_{C_{m,n}}^{j}\right)\left(T_{m-1,n-1}^{j} - T_{m,n}^{j}\right) \right] \right\} \quad (3)$$

2.6 Insulation Region (Case 4)

In this region the heat is transferred only by conduction as shown in Fig. 8, the following expression is obtained for heat flow in the insulation:

$$T_{m,n}^{j+1} = T_{m,n}^{j} + \frac{\Delta t}{\left[\rho_c C_c\right]_{m,n}^{j} \Delta h_g} \cdot \frac{1}{2} \left\{ \left[\left(K_{C_{m-1,n-1}}^{j} + K_{C_{m,n}}^{j}\right)\left(T_{m-1,n-1}^{j} - T_{m,n}^{j}\right) \right] + \right.$$

$$\left[\left(K_{C_{m,n}}^{j} + K_{C_{m-1,n+1}}^{j}\right)\left(T_{m-1,n+1}^{j} - T_{m,n}^{j}\right) \right] + \left[\left(K_{C_{m+1,n-1}}^{j} + K_{C_{m,n}}^{j}\right)\left(T_{m+1,n-1}^{j} - T_{m,n}^{j}\right) \right] +$$

$$\left. \left(K_{C_{m-1,n-1}}^{j} + K_{C_{m,n}}^{j}\right)\left(T_{m-1,n-1}^{j} - T_{m,n}^{j}\right) \right\} \quad (4)$$

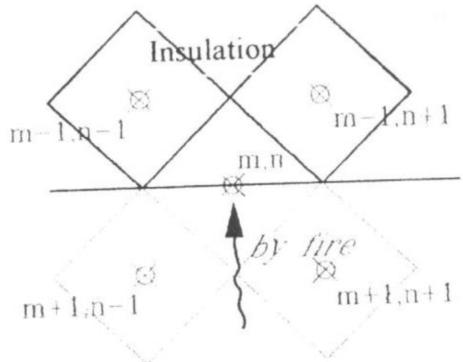

Fig. 7 Case 3

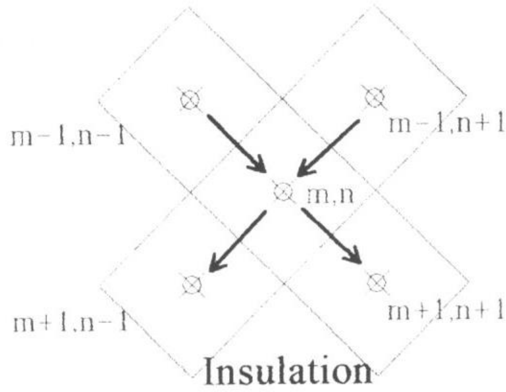

Fig. 8 Case 4

2.7 Insulation – Steel Boundary (Case 5)

The heat is transferred only by conduction shown in Fig. 9 but through two different materials which are insulation and steel:

$$T_{m,n}^{j+1} = T_{m,n}^{j} + \frac{\Delta t}{\left[\rho_c C_c + \rho_s C_s\right]_{m,n}^{j} \Delta h_g} \cdot \frac{1}{2} \left\{ \left[\left(K_{C_{m-1,n+1}}^{j} + K_{C_{m,n}}^{j} \right) \left(T_{m-1,n+1}^{j} - T_{m,n}^{j} \right) \right] + \left[\left(K_{C_{m,n}}^{j} + K_{C_{m-1,n-1}}^{j} \right) \left(T_{m-1,n-1}^{j} - T_{m,n}^{j} \right) \right] + \left[\left(K_{S_{m+1,n-1}}^{j} + K_{S_{m,n}}^{j} \right) \left(T_{m+1,n-1}^{j} - T_{m,n}^{j} \right) \right] + \left[\left(K_{S_{m+1,n+1}}^{j} + K_{S_{m,n}}^{j} \right) \left(T_{m+1,n+1}^{j} - T_{m,n}^{j} \right) \right] \right. \tag{5}$$

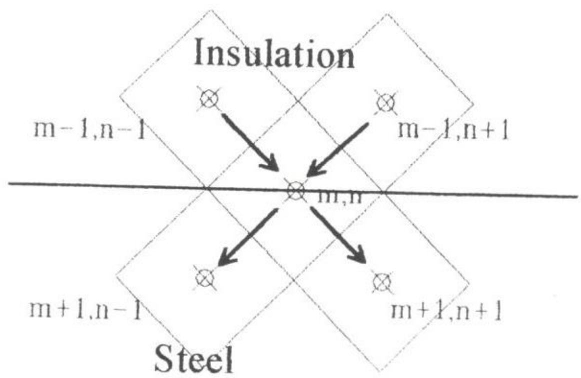

Fig. 9 Case 5

2.8 Insulation – Steel Boundary (Case 6)

The heat transfer expression for conduction through two different materials is obtained for this boundary condition (see Fig. 10).

$$T_{m,n}^{j+1} = T_{m,n}^{j} + \frac{\Delta t}{\left[\rho_c C_c + \rho_s C_s\right]_{m,n}^{j} \Delta h_g} \cdot \left\{ \frac{1}{2} \left[\left(K_{C_{m-1,n+1}}^{j} + K_{C_{m,n}}^{j} \right) \left(T_{m-1,n+1}^{j} - T_{m,n}^{j} \right) \right] + \right.$$
$$\left[\left(K_{C_{m,n}}^{j} + K_{C_{m+1,n+1}}^{j} \right) \left(T_{m+1,n+1}^{j} - T_{m,n}^{j} \right) \right] + \left[\left(K_{S_{m+1,n-1}}^{j} + K_{S_{m,n}}^{j} \right) \left(T_{m+1,n-1}^{j} - T_{m,n}^{j} \right) \right] +$$
$$\left[\left(K_{S_{m-1,n-1}}^{j} + K_{S_{m,n}}^{j} \right) \left(T_{m-1,n-1}^{j} - T_{m,n}^{j} \right) \right] \qquad (6)$$

2.8 Insulation – Steel Boundary (Case 7)

Similarly, the heat transfer expression for conduction as shown in Fig. 11 through two different materials is obtained.

$$T_{m,n}^{j+1} = T_{m,n}^{j} + \frac{\Delta t}{\left[\rho_c C_c + \rho_s C_s\right]_{m,n}^{j} \Delta h_g} \bullet \frac{1}{2} \left\{ \left[\left(K_{S_{m-1,n-1}}^{j} + K_{S_{m,n}}^{j} \right) \left(T_{m-1,n-1}^{j} - T_{m,n}^{j} \right) \right] + \right.$$
$$\left[\left(K_{S_{m,n}}^{j} + K_{S_{m-1,n+1}}^{j} \right) \left(T_{m-1,n+1}^{j} - T_{m,n}^{j} \right) \right] + \left[\left(K_{C_{m+1,n-1}}^{j} + K_{C_{m,n}}^{j} \right) \left(T_{m+1,n-1}^{j} - T_{m,n}^{j} \right) \right] +$$
$$\left[\left(K_{C_{m+1,n+1}}^{j} + K_{C_{m,n}}^{j} \right) \left(T_{m+1,n+1}^{j} - T_{m,n}^{j} \right) \right] \qquad (7)$$

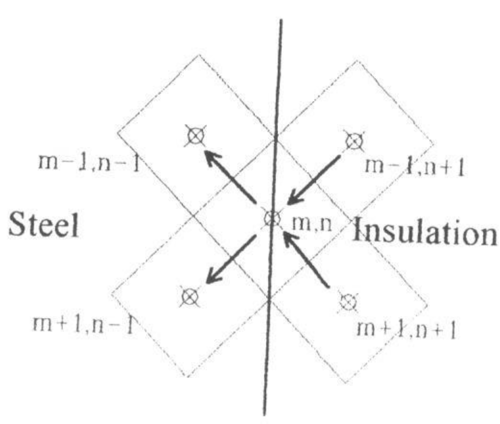

Fig. 10 Case 6

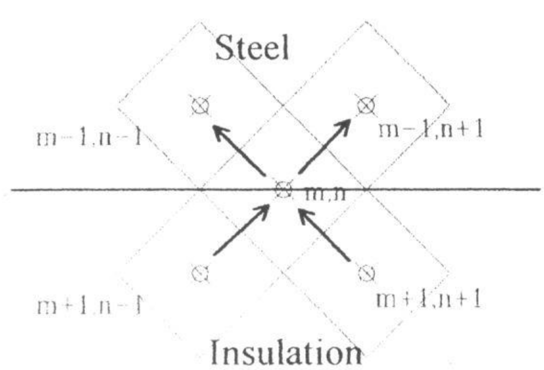

Fig. 11 Case 7

2.8 Steel Region

This boundary involves heat conduction in steel only as shown in Fig. 12.

$$T_{m,n}^{j+1} = T_{m,n}^{j} + \frac{\Delta t}{\left[\rho_s C_s\right]_{m,n}^{j} \Delta h_g} \bullet \frac{1}{2} \left\{ \left[\left(K_{S_{m-1,n-1}}^{j} + K_{S_{m,n}}^{j} \right) \left(T_{m-1,n-1}^{j} - T_{m,n}^{j} \right) \right] + \right.$$
$$\left[\left(K_{S_{m,n}}^{j} + K_{S_{m-1,n+1}}^{j} \right) \left(T_{m-1,n+1}^{j} - T_{m,n}^{j} \right) \right] + \left[\left(K_{S_{m+1,n-1}}^{j} + K_{S_{m,n}}^{j} \right) \left(T_{m+1,n-1}^{j} - T_{m,n}^{j} \right) \right] +$$
$$\left. \left[\left(K_{S_{m+1,n+1}}^{j} + K_{S_{m,n}}^{j} \right) \left(T_{m+1,n+1}^{j} - T_{m,n}^{j} \right) \right] \right\} \qquad (8)$$

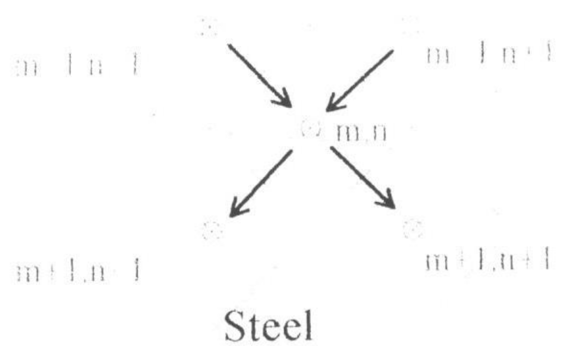

Fig. 12 Case 8

3.0 STABILITY CRITERION

In order to ensure that any error existing in the solution at some time level will not be amplified in subsequent calculations, a stability criterion has to be satisfied which, for a selected value of $\Delta\xi$, limits the maximum of time step Δt. Following the method described in by Dusinberre[3], it can be derived that, for the fire-exposed column, the criterion of stability is most restrictive along the boundary between fire and insulation. It is given the condition:

$$\Delta t \leq \frac{(\Delta\xi)^2}{\dfrac{4K_{\max} + 2\sqrt{2} \cdot \Delta\xi \cdot h_{\max}}{(\rho_c C_c)_{\min}}} \qquad (9)$$

where the maximum value of the coefficient of heat transfer during exposure to the standard fire (h_{max}) is approximately 3 x 10^6 J/m^{2}h°C (147 Btu/ft^{2}h°F).

4.0 STRENGTH MATHEMATICAL MODEL

The strength of the column during exposure to fire can be calculated by a method based on a load deflection analysis. In this method, the columns, which are fixed at the ends during the tests, are idealised as pin-ended columns of length *KL*. In a previous study, it was estimated that for columns tested fixed at the ends, the effective length *KL* is about 2m.

In the calculation of the column strength, the following assumptions were made:

1. plane sections remain plane, and
2. the insulation does not contribute to carrying the load.

The load on the column is intended to be concentric. Due to imperfections of the column and loading device, a small eccentricity exists. Therefore in the calculations a very small initial load eccentricity will be assumed. After runs of the computer program showed that for small eccentricities up to about 10mm, the influence of eccentricity on fire resistance is very small, a value of 0.2mm reflecting a nearly concentric load, was selected for the initial eccentricity.

The curvature of the column is assumed to vary from pin-ended to mid-height according to a straight line relation, as illustrated in Fig. 13. For such a relation the deflection at mid-height y, in terms of the curvature χ of the column at this height, can be given by

$$y=\chi \cdot \frac{(KL)^2}{12} \tag{10}$$

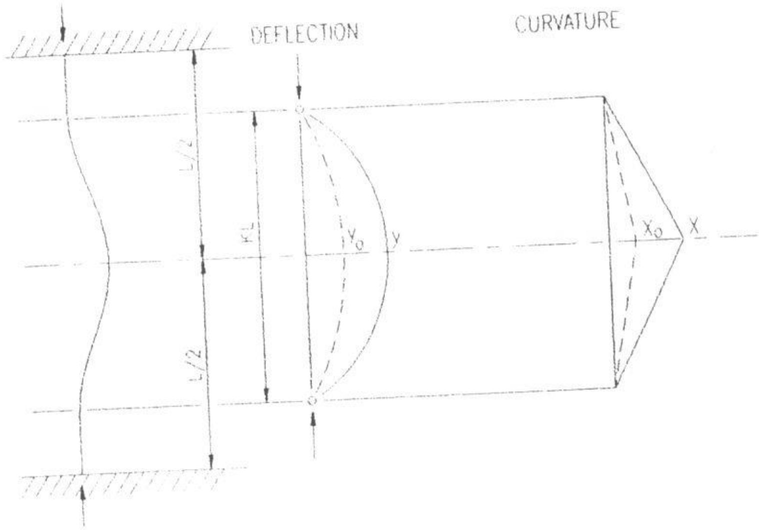

Fig. 13 Curvature of the Column

4.1 Strains

The strain in an element of the steel can be given as the sum of the axial strain of the column ε_A, the strain due to bending of the column, ε_B and the thermal expansion of the steel, ε_T. For any given curvature, and thus for any given deflection at mid-height, the axial strain, ε_A is varied until the internal moment at the mid-section is in equilibrium with the applied moment given by the product

load x (deflection + eccentricity)

For a radius of curvature, ρ and horizontal distance, Z_s from steel elements to the x-axis, the bending strain is given by

$$\varepsilon_b = \frac{Z_s}{\rho} \tag{11}$$

Thermal strain due to expansion is given by

$$\varepsilon_T = \alpha_s \cdot \Delta T$$

For the steel at the right of the x-axis, the strain $(\varepsilon_s)_R$ is given by

$$\left(\varepsilon_S\right)_R = -\left(\varepsilon_T\right)_S + \varepsilon + {}^{z_s}\!/_{\rho} \quad (12)$$

For the steel elements at the left of the x-axis the strain $(\varepsilon_s)_L$ is given by

$$\left(\varepsilon_S\right)_L = -\left(\varepsilon_T\right)_S + \varepsilon - {}^{z_s}\!/_{\rho} \quad (13)$$

4.2 Yield Strength

The yield strength of steel is the point at which material is considered as having reached its highest loading capacity in Structural design. At elevated temperature, the yield strength of all materials will deteriorate rendering the structure useless as a load supporting mechanism.

If . $0 < T \leq 600°C$

then
$$f_{yT} = \left[1 + \frac{T}{900 \cdot \ln\left(T/1750\right)}\right] \cdot f_{yO} \quad (14)$$

If $600 < T < 1000°C$

then
$$f_{yT} = \left[\frac{340 - 0.34 \cdot T}{T - 240}\right] \cdot f_{yO} \quad (15)$$

4.3 Modulus of Elasticity

According to the modulus of elasticity, the expansion of material is linear when load is applied and it will revert to its original size when the load is removed. At this range, loaded material will not deformed and will retain all its original properties including size.

If $0 < T \leq 600°C$

then
$$E_T = \left[1 + \frac{T}{2000 \cdot \ln\left(T/1100\right)}\right] \cdot E_O \quad (16)$$

If $600 < T < 1000°C$

then $$E_T = \left[\frac{690-0.69\cdot T}{T-53.5}\right]\cdot E_O \tag{17}$$

4.4 Elastic Curve and Proportional Limits

The expansion of steel is according to the elastic curve until the proportional limit. After this point the expansion is non-linear and subsequently, at this range material will suffer permanent deformations even though the load is later removed. This limit is related to the steel temperature and its value changes with temperature.

The proportional limit is given by,

$$\varepsilon_p = \frac{0.975\cdot f_{yT} - 12.5\cdot {(f_{yT})^2}/{E_T}}{E_T - 12.5\cdot f_{yT}} \tag{18}$$

4.5 Stress and Strain Relationship

If $\varepsilon_s \leq \varepsilon_p$ then $f_T = E_T \cdot \varepsilon_s$ (19)

If $\varepsilon_s \geq \varepsilon_p$ then $f_T = 12.5\, f_{yT}\, \varepsilon_s + 0.975\, f_{yT} - 12.5\, (f_{yT})^2 / E_T$ (20)

4.6 Loads and Moments in Steel

The total load in the steel column is given by:

$$2\left\{\sum_{n=1}^{N}(f_{TR})_n\cdot A_S + \sum_{n=1}^{N}(f_{TL})_n\cdot A_S\right\} \tag{21}$$

The total moment in the steel column is given by:

$$2\left\{\sum_{n=1}^{N}(f_{TR})_n \cdot A_S \cdot Z_n + \sum_{n=1}^{N}(f_{TL})_n \cdot A_S \cdot (-Z_n)\right\} \tag{22}$$

5.0 CONCLUSION

With the aid of Eqn. 1 to Eqn. 22, the stresses at mid-section in the steel elements can be calculated for any value of the axial strain and curvature. From these stresses, the load that each element carries and its contribution to the internal moment at mid-section can be derived. By adding the loads and moment, the load that the column carries and the total internal moment at mid-section can be calculated. In this way, a load deflection curve can be calculated for specific times during the exposure to fire. From these curves the strength of the column, i.e. the maximum that the column can carry, can be determined for each time. The change of column strength during exposure to fire was also calculated. The fire resistance of the column is derived by calculating the strength i.e. the maximum load that the column can carry at several consecutive time during the exposure to fire. This strength reduces gradually with time. At a certain point the strength become so low that it no longer sufficient to support the load, and the column fails. The time to reach this failure point is the fire resistance of the column.

From the above-mentioned equations, from Eqns. (1 to 22), two mathematical models will be developed by using Finite Difference technique. The models will then be converted into a computer program using Microsoft Fortran.

NOMENCLATURE

A_{fs} : surface area of the element exposed to fire $= 2(\Delta h_g)(1.0)$

A_{EL} : area of element

A_s : area of steel element

C : thermal capacity

E_T : modulus at temperature T

E_o : modulus at room temperature

f_{yo}	: yield strength at room temperature
f_{yt}	: yield strength at temperature T
f_{TR}	: stress in the steel element at right side of x-axis
f_{TL}	: stress in the steel element at left side of x-axis
h_{max}	: maximum value of the coefficient of heat transfer during exposure to the standard fire = 3 x 10^6 J/m^{2}h°C (147 Btu/ft^{2}h°F).
K_s	: thermal conductivity of steel
K_c	: thermal conductivity of coating (insulation)
KL	: effective length
M	: maximum node along X axis
n	: nth element
N	: maximum node along Y axis
N	: total number of steel elements
q_r	: heat transferred by radiation , J/m.hr
ΔT	: temperature rise in the element
Δt	: time step
T	: temperature
T	: temperature of element at current time step
T^{j+1}	: the next time step
T^j	: current time step
y	: deflection at mid-height
Z_n	: distance of steel element from x-axis
Z_s	: horizontal distance from steel elements to the x-axis
ε_s	: strain in steel at particular time step
ε_p	: strain in steel below the yield limit
$(\varepsilon_s)_R$	: the strain of steel element at the right of the x-axis
$(\varepsilon_s)_L$	: the strain of steel element at the left of the x-axis
α_s	: coefficient of thermal expansion of steel
ρ	: radius of curvature

ε_A : axial strain

ε_B : strain due to bending of the column

ε_T : thermal expansion of the steel

χ : curvature of the column

REFERENCES

1. El-Shayeb, Mohamed, Fire-Resistance of Concrete-Filled and Reinforced concrete columns, PhD. Thesis, University of New Hampshire, USA, May 1986.

2. Lie, T. T. ,Temperature of Protected Steel in Fire, Behaviour of Structural Steel in Fire, Ministry of Technology and Fire Offices, Committee Joint Fire Research Organisation Symposium No. 2, H. M. S. O., London, 1968.

3. Lie, T. T., Feasibility of Determining the Equilibrium Moisture Condition in Fire Resistance Test Specimens by Measuring their Electrical-Resistance, Building Research Note No. 75, Division of Building Research, NRC, Ottawa, 1971.

4. Dusinberre, G. M., Heat Transfer Calculations by Finite Differences, International Textbook Company, Scranton, Pennsylvania, 1961.

5. Harmathy, T. Z., A treatise on Theoretical Fire Endurance Rating, American Society for Testing Materials, Special Technical Publication No. 301, 1961, pp. 10-40.

6. Harmathy, T. Z. and Lie, T. T., Experimental Verification of the Rule of Moisture Moment. Fire Technology, Vol. 7, 1964 p. 17.

7. Bibliography Bardell, K., Spray-Applied Fire Resistive Coatings for Steel Building Columns, Fire Resistive Coatings: The Need For Standards, ASTM STP 826 Morris Lieff and F.M. Stumpf, eds., American Society for Testing and Materials, 1983, 40-55.

8. Standard Methods of Fire Tests of Building Construction and Materials, ASTM Designation E119-69, 1969 Book of ASTM Standards, Part 14, pp. 436-452.

9. British Iron Steel Research Assoc., Physical Constants of Some Commercial Steels at Elevated Temperature., Butterworths Sci. Publ., London, 1953.

10. Fujii, S., The Theoretical Calculation of Temperature-rise of Thermally Protected Steel Column Exposed to the Fire, Building Research Institute Occasional Report No. 10, Tokyo, 1963.

11. Emmons, H. W., The Numerical Solution of Heat Conduction problems., Transactions of the American Society of Mechanical Engineers, Vol. 65, 1943, pp. 607-615.

12. Thrinks, W. and Mawhinney, M. W., Industrial Furnaces, John Wiley and Sons, Inc., New York, 1986.

13. Law, M. Structural Fire Protection in the Process Industry Building, Vol. 216, No. 29, 1969, pp. 86-90.

14. Rains, W.A., Evaluation on Existing Fire Protection Materials, Phase 1 Report, Presented to the American Iron and Steel Institute Fire Technology Subcommittee, 1973.

15. Stumpf, Frank M., Spray-Applied Fibrous Materials and Fire Resistive Coatings, Presented to the ASTM, 1984.